Published in final edited form as:
Magn Reson Imaging Clin N Am. 2008 November ; 16(4): 697–x. doi:10.1016/j.mric.2008.07.005.

ADVANCES IN MR SPECTROSCOPY OF THE PROSTATE

John Kurhanewicz, Ph.D.[a] and **Daniel B Vigneron**[b]
University of California, San Francisco, CA

[a]Professor of Radiology, Urology, and Pharmaceutical Chemistry University of California, San Francisco Byers Hall, Room 203E 1700 4th Street, Box 2520 San Francisco, CA 94158 Tel: (415) 514-9711 Fax: (415) 514-4714 john.kurhanewicz@radiology.ucsf.edu

[b]Professor of Radiology University of California, San Francisco Byers Hall, Room 102 1700 4th Street, Box 2520 San Francisco, CA 94158 Tel: (415) 476-3343 Fax: (415) 514-4714 Daniel.Vigneron@radiology.ucsf.edu

SYNOPSIS

Commercial MRI/MRSI packages for staging prostate cancer on 1.5 T MR scanners are now available and the technology is becoming mature enough to begin assessing it's clinical utility in selecting, planning and following prostate cancer therapy. Prior to therapy, Studies have demonstrated that 1.5T MRI/MRSI has the potential to significantly improve the local evaluation of prostate cancer presence and volume and has been shown to have a significant incremental benefit in the prediction of pathological stage when added to clinical nomograms. After therapy, two metabolic biomarkers of effective (metabolic atrophy) and ineffective therapy (3 or more voxels of elevated choline to creatine) have been identified and are being validated with 10 year outcomes. Recent studies have also shown that accuracy can be improved by performing MRI/MRSI at higher magnetic field strengths (3T), using of more sensitive hyperpolarized ^{13}C MRSI techn1ques and through the addition of other functional MR techniques, namely diffusion-weighted imaging (DWI) and dynamic contrast-enhanced (DCE) MRI.

Keywords

prostate cancer; ^{1}H magnetic resonance spectroscopic imaging (MRSI); hyperpolarized ^{13}C MRSI; citrate; choline; polyamines

INTRODUCTION

While Magnetic Resonance Imaging (MRI) traces anatomy, ^{1}H Magnetic Resonance Spectroscopic Imaging (MRSI) is used to spatially detect deviations from normal biochemistry that occurs in tumor tissue. Specifically, MR anatomic images, especially high spatial resolution combined endorectal coil pelvic phased array MR images, provide an excellent depiction of prostatic anatomy with regions of healthy prostate tissue demonstrating higher signal intensity than prostate cancer on T2-weighted images (1). MRSI provides a non-invasive

[a]Corresponding author for proofs and reprints: John Kurhanewicz, Ph.D. University of California, San Francisco Byers Hall, Room 203E 1700 4th Street, Box 2520 San Francisco, CA 94158 Tel: (415) 514-9711 Fax: (415) 514-4714 john.kurhanewicz@radiology.ucsf.edu.

method of detecting small molecular biomarkers (choline-containing metabolites, polyamines and citrate) within the cytosol and extracellular spaces of the prostate and is performed in conjunction with high-resolution anatomic imaging (MRI) (2) (Figure 1).

The robust acquisition of prostate MRSI requires very accurate volume selection and efficient outer volume suppression (3-5). The resonances for citrate, choline, creatine and polyamines occur at distinct frequencies or positions in the spectrum, although the peaks for choline, creatine and polyamines overlap at 1.5T (Figure 1C and D). The areas under these signals are related to the concentration of the respective metabolites, and changes in these concentrations can be used to identify cancer with good specificity (6,7). Specifically, in spectra taken from regions of prostate cancer (Figure 1D), citrate and polyamines are significantly reduced or absent, while choline is elevated relative to spectra taken from surrounding healthy peripheral zone tissue (Figure 1C).

Commercial combined 1.5T MRI/MRSI exams are currently available and a growing amount of published data has demonstrated that the metabolic biomarkers, choline, citrate and polyamines, provided by 3-D ^{1}H MRSI combined with the anatomical information provided by MRI can significantly improve the detection and characterization of prostate cancer in individual patients (8,9) (Figure 1). Recent patient studies have also demonstrated that the detection and characterization of prostate cancer can be improved through the addition of more sensitive spectroscopic imaging techniques (hyperpolarized ^{13}C MRSI) (10), diffusion-weighted imaging (DWI), dynamic contrast enhanced (DCE) imaging, and by performing the multi-parametric imaging exam at 3T (9). In this chapter, the current status and recent advances in MRI/MRSI of prostate cancer will be described.

Unique Metabolism of the prostate

The metabolic changes observed by ^{1}H MRSI take advantage of the well documented unique metabolism of healthy prostate epithelial cells which have the specialized function of synthesizing and secreting large amounts of citrate which is dramatically reduced or lost in prostate cancer (11-14). The decrease in citrate with prostate cancer is due both to changes in cellular function (15) and changes in the organization of the tissue, resulting in a loss of its characteristic ductal morphology (16,17). The loss of citrate in prostate cancer is intimately linked with changes in zinc levels that are extraordinarily high in healthy prostate epithelial cells (13,18). In healthy prostatic epithelial cells, the presence of high levels of zinc inhibit the enzyme aconitase, thereby preventing the oxidation of citrate in the Krebs' cycle (13,18). Costello and Franklin, have shown that these elevated levels of zinc are primarily due to increased expression of ZIP-type plasma membrane Zn uptake transporters (primarily Human ZIP-1) (14). Human ZIP-1 is reduced and zinc levels are dramatically reduced in prostate cancer and the malignant epithelial cells and there exists evidence that the loss of the capability to retain high levels of zinc is an important factor in the development and progression of prostate cancer (13,18). It is also believed that the transformation of prostate epithelial cells to citrate-oxidizing cells, which increases energy production capability, is essential to the process of malignancy and metastasis (12).

The elevation of choline-containing metabolites [phosphocholine (PC), glycerophosphocholine (GPC), free choline (Cho)] and the over and under-expression of key enzymes in phospholiopid membrane sysnthesis and degradation, specifically choline kinase and a number of the phospholipases, have been associated with the presence, progression and therapeutic response of a variety of human cancers including prostate (8,19-21). Specifically, High Resolution Magic Angle Spinning (HR-MAS) spectroscopic studies of ex vivo surgical prostate tissues demonstrated elevated levels of ethanolamine and choline containing compounds and that elevated PC was the most robust predictor of prostate cancer (22). In ^{1}H MRSI studies of prostate cancer patients, the elevation of the in vivo "choline" resonance has

also been the most specific biomarker of prostate cancer presence(8), and both in vivo and ex vivo spectroscopic studies have shown that the degree of elevation of choline roughly correlates with Gleason score (8).

Healthy prostate epithelial cells also contain very high concentrations of polyamines, particularly spermine (8,23,24). Similar to citrate, polyamines are dramatically reduced in prostate cancer and this reduction is associated with significant changes in the levels of expression of polyamine metabolism regulatory genes (8,23). Ornithine decarboxylase catalyzes the first step of spermine synthesis, and has been found to be over-expressed in prostate cancer (23). The polyamines spermidine and spermine have been implicated or involved in a wide variety of physiologic processes, most of which are closely related to cell proliferation (25). The polyamines also exert diverse effects on protein synthesis and act as inhibitors of numerous enzymes including several kinases (25). However, similar to citrate high levels of spermine are found in the prostatic ducts and the observed changes in spermine may also be due to the loss of ductal morphology or a reduction in the secretion of polyamines in cancer (26).

CLINICAL APPLICATIONS OF 1.5T MRI/MRSI

■ Detection and Localization of Cancer Within the Prostate

In clinical practice, reliable detection and localization of often small regions of prostate cancer is of increasing therapeutic importance due to the emergence of “active surveillance” and focal ablative therapy (27). In addition, tumor localization has been related to the risk of post-prostatectomy tumor recurrence, with a higher risk when surgical margins are positive at the base than at the apex (6). It has been demonstrated in multiple studies that MRSI can be used to improve the ability of MRI to identify the location and extent of cancer within the prostate (6,7,28-31) (Figure 1). A study of 53 biopsy proven prostate cancer patients prior to radical prostatectomy and step-section pathologic examination demonstrated a significant improvement in cancer localization to a sextant biopsy of the prostate (left and right – base, midgland, and apex) of the prostate using combined MRI/MRSI versus MRI alone. A combined positive result from both MRI and MRSI indicated the presence of tumor with high specificity (91%) while high sensitivity (95%) was attained when either test alone indicated the presence of cancer (7). In another study it was found that the addition of a positive sextant biopsy finding to concordant MRI/MRSI findings further increased the specificity (98%) of cancer localization to a prostatic sextant, whereas high sensitivity (94%) was again obtained when any of the tests alone were positive for cancer (6). However, more recent studies in early stage prostate cancer patients have indicated that combined 1.5 MRI/MRSI does poorly at detecting and localizing small low grade tumors (28,31,32). One recent study demonstrated that overall sensitivity of MR spectroscopic imaging was 56% for tumor detection, increasing from 44% in lesions with Gleason score of 3 + 3 to 89% in lesions with Gleason score greater than or equal to 4 + 4 (32). The inability to detect small low grade tumors by 1.5T MRSI is primarily due to averaging of surrounding benign tissue in spectroscopic volumes containing cancer due to the spatial resolution of 1.5T MRSI (0.34 cc, ≈ 7mm on a side). In a recent multicenter trial of prostate MRI/MRSI (ACRIN 6659), the clinical downstaging (smaller lower grade disease) of prostate cancer in patients going on for surgery had a significant impact on the sensitivity and specivicity of tumor detection. Complete data were available for 110 patients. MRI alone and combined MRI/MRSI were of similar poor accuracy in peripheral zone tumor localization (AUC of 0.60 versus 0.58, respectively, $P > 0.05$) (33). At 3T, spatial resolution of MRSI can be increased ≈ 2 fold (0.16 cc, ≈ 5 mm on a side) in the same acquisition time (Figure 2), and this will be clearly needed for the imaging of men with early stage, small volume (<0.5 cc) prostate cancer.Another study demonstrated that DCE MRI can detect and determine the volume of smaller foci of prostate cancer with greater overall accuracy than MRI/MRSI. Sensitivity, specificity, and positive and negative predictive values for cancer detection by

DCE MRI were 77%, 91%, 86% and 85% for foci greater than 0.2 cc, and 90%, 88%, 77% and 95% for foci greater than 0.5 cc, respectively (34).

■ Tumor Volume Estimation

The pathologic finding that larger tumors are more likely to be of an advanced stage suggests measurement of tumor volume may provide important information on prognosis that is independent of direct morphologic assessment of extracapsular extension (35). This has important implications for the potential prognostic role of imaging in prostate cancer, since: "it is beyond the capability of any current imaging study to detect microscopic local tumor extension"(36). Two recent studies suggest that MRI/MRSI and DCE MRI may non-invasively provide estimates of cancer volume at diagnosis. One study investigated the estimation of prostate cancer tumor volume by endorectal MRI and MRSI in 37 patients who were scanned prior to radical prostatectomy (31). This study demonstrated that for nodules greater than 0.5 cm^3, tumor volume measurements by MRI, MRSI, and combined MRI and MRSI were all positively correlated with histopathologic volume (Pearson's correlation coefficients of 0.49, 0.59, and 0.55, respectively), but only measurements by MRSI and combined MRI/MRSI reached statistical significance ($p < 0.05$). The findings also suggested that the addition of MRSI to MRI increased the overall accuracy of prostate cancer tumor volume measurement, although measurement variability still limited consistent quantitative tumor volume estimation, particularly for small tumors (under 0.5 cm^3).

■ Detection of High Grade Prostate Cancer

The histology of prostate cancer is variable, ranging from well (Gleason score $\leq$ 3+4) to poorly differentiated (Gleason score 4/3, 8, 9, 10) (37). The evaluation of the dominant histological pattern is important, because poorly differentiated tumors are more aggressive, and are predictive of cancer stage. Specifically, in a study of 113 patients undergoing radical prostatectomy (38), 63% of patients with a Gleason score of 6 or less had organ-confined disease, compared to 33% of patients with a Gleason score of 7 and 0% of patients with a Gleason score of 8. Limitations of the Gleason score are clustering of assigned values to 6 and 7, and high inter-observer variability (39). MRSI may be able to provide an non-invasive assessment of cancer grade for all of the cancer foci within the prostate, potentially with reduced inter-observer variaility and grade clustering. Early biochemical studies have indicated that citrate levels in prostatic adenocarcinomas are grade dependent, with citrate levels being low in well-differentiated, low-grade prostatic cancer and effectively absent in poorly-differentiated high-grade prostatic cancer (40,41). More recent proton high resolution magic angle spinning (HR-MAS) spectroscopy studies of intact human prostate tissues have demonstrated a significant, grade dependent elevation of choline and ethanolamine containing phospholipid membrane metabolites in prostate cancer (19,20). In a MRI/MRSI study of 32 patients prior to surgery, there was a statistically significant relationship between the choline and creatine to citrate ratio and Gleason score (42). However, these results were obtained for lesions that were identified on pathology and that also had a concordant MRI finding of low T_2 signal intensity. In a study of 123 patients, where this approach was not taken, there was only a trend in the choline+creatine/citrate ratio with Gleason score. In clinical practice, the pathologic location of the lesion is not known and MRSI voxels contain a complex mixture of malignant and benign tissue types which reduce its ability to determine cancer grade (32). This can be improved with the improved spectral resolution obtainable on 3T MRSI.

■ Predicting Organ Confined (No extracapsular extension or seminal vesicle invasion) Prostate Cancer

A more accurate prediction of organ confined prostate cancer at the time of diagnosis would allow the determination of whether "focal therapy" is appropriate for a given patient. The use

of T_2-weighted fast spin echo imaging and a pelvic phased-array incorporating an endorectal coil can markedly improved the evaluation of extracapsular extension (ECE: accuracy = 81%; sensitivity = 84%; and specificity = 80%) and seminal vesicle invasion (SVI: accuracy = 96%; sensitivity = 83%; and specificity = 98%) thereby improving the staging of prostatic cancer (43). However, the detection of ECE and SVI by MRI is becoming more difficult since men are being diagnosed at earlier stages of disease, and because the microscopic spread of cancer through the prostatic capsule or into the seminal vesicles cannot be directly seen on MRI. Two studies have suggested that the addition of MRSI to MRI data can improve prostate cancer staging. In one study of 53 patients with early stage prostate cancer, tumor volume estimates based on MRSI findings were combined with MRI criteria (44) in order to assess the ability of combined MRI/MRSI to predict extracapsular cancer spread. It was found that tumor volume per lobe estimated by MRSI was significantly ($p<0.01$) higher in patients with ECE than in patients without ECE. Moreover the addition of a MRSI estimate of tumor volume to MRI findings for ECE (43) improved the diagnostic accuracy and decreased the inter-observer variability of MRI in the diagnosis of extracapsular extension of prostate cancer (44).

■ Adding MRI/MRSI to Clinical Nomograms

An important advance in the staging of prostate cancer has been the development of multivariable risk prediction instruments such as the Partin tables (45) and nomograms, which combine clinical stage, serum PSA levels, and grade of biopsies results to predict at the time of diagnosis the pathologic stage of the cancer and indolent disease, respectively (46,47). Recent studies have demonstrated that addition of 1.5T MRI/MRSI findings can to significantly improve the predictive ability of these nomograms. In a study of 24 prostate cancer patients prior to radical prostatectomy the addition of endorectal MR imaging results contributed significant incremental value to the biopsy based nomograms for predicting SVI (48). It was found that the nomogram plus endorectal MR imaging (0.87) had a significantly larger ($P< 0.05$) AUC than either endorectal MR imaging alone (0.76) or the nomogram alone (0.80) (48). In another study of 383 prostate cancer patients prior to radical prostatectomy, 1.5T MRI/MRSI data were added to a biopsy based staging nomogram for predicting organ-confined prostate cancer (OCPC, no ECE or SVI) in order to assess its incremental value. The increase in predictive accuracy provided by the addition of 1.5T MR/MRSI findings were significant in all patient risk groups but were greatest in the intermediate- and high-risk groups ($p < .01$ for both) (49).

■ Predicting Indolent Disease

Due to increased screening using serum prostate specific antigen (PSA) and extended-template transrectal ultrasound (TRUS) guided biopsies, thousands of patients with prostate cancer are being identified at an earlier and potentially more treatable stage (50). However, the risk of over-detection, detecting a cancer which would not become clinically significant during that patient's lifetime if left untreated, has been estimated to vary between 15% and 84% (51-53). Therefore there is an increased interest in "active surveillance", but clinical parameters alone are not sufficient to predict a benign disease course. A recent study suggests that the addition of MRI/MRSI data to clinical parameters can improve this prediction. In a study of 220 patients prior to surgery, the addition of MRI (AUC – 0.803) and 1.5T MRI/MRSI (AUC 0.854) to biopsy based nomograms (basic – AUC 0.57, comprehensive 0.73) was found to significantly improve the prediction of indolent prostate cancer using a surgical definition of indolent disease (no SVI, ECE and < 0.5 cm3 of cancer with no pattern 4 or 5 cancer) as the standard of reference.

■ Cancer Detection in Men with Prior Negative Biopsies

Another important group of patients being referred for an MRI/MRSI exam prior to therapy is comprised of men who have elevated or rising PSA levels but negative TRUS guided biopsies.

These patients tend to have very enlarged central glands due to BPH, which present sampling problems for TRUS guided biopsies, or they have cancers in difficult locations to biopsy such as the apex or in the lateral or anterior locations within the prostate (54). A recent publication has demonstrated that MRI/MRSI can improve the identification of regions of cancer for targeting of TRUS guided biopsies in patients with prior negative TRUS biopsy (55,56).

■ Therapeutic Selection and Planning

Several possible roles for MRI and MRSI have been suggested in radiation treatment planning. Staging by MRI/MRSI at diagnosis has been found to be of incremental prognostic significance in patients with moderate and high-risk tumors going on for radiation therapy (57). Specifically, the finding of more than 5 mm of extracapsular extension prior to radiation seems to be of particular negative prognostic significance, and the latter group may be candidates for more aggressive supplemental therapy (57). For the patient in Figure 3, the MRI/MRSI findings were concordant, indicating a large volume of T_2 hypointensity (Figures 1A, red arrows) and associated abnormal spectroscopic voxels (significantly elevated choline and reduced polyamine and citrate (Figure 3A, red arrows) bilaterally at the midgland and apex of the prostate. Additionally, there was a mild bulge of the prostate and irregularity of the prostatic capsule in the left midgland indicative of extracapsular extension. However, there was no evidence of seminal vesicle invasion or pelvic lymphadenopathy within the pelvis. Based on these findings it was clear that aggressive therapy would be necessary. The patient subsequently underwent high dose rate brachytherapy combined with 22 sessions of external beam radiation therapy, and neoadjuvant androgen deprivation therapy.

Using fiducial markers and image fusion software, it has been shown that CT overestimates the clinical target volume by 34% when compared to MRI (58), and that dose-volume planning with MRI would decrease radiation dose to the bladder, rectum, and femoral heads. This result is hardly unexpected, given the limited soft tissue contrast of CT in the prostate and perineum, particularly when CT is performed without intravenous contrast enhancement, as is the usual protocol for radiation planning CT scans. Several recent research studies have directly integrated MRI/MRSI data into the radiation treatment plan in order to optimize radiation dose selectively to regions of prostate cancer using either Intensity Modulated Radiotherapy (IMRT) (59-61) or brachytherapy (62-65), however, this is not being done in routine clinical practice.

■ MRI and MRSI in post-treatment follow-up

A growing numbers of patients receiving a MRI/MRSI are referred for suspected local cancer recurrence after various therapies (hormonal deprivation therapy, radiation therapy, cryosurgery and radical prostatectomy). Recurrent cancer is typically suspected in these patients due to a detectable or rising PSA. However, the use of PSA testing to monitor therapeutic efficacy is not ideal since PSA is not specific for prostate cancer, and it can take two years or more for PSA levels to reach a nadir following radiation therapy (both external beam and brachytherapy) (66,67). Further, the interpretation of PSA data is more complicated for patients undergoing therapies such as hormone deprivation therapy that have a direct effect on the production of PSA. Conventional imaging methods including TRUS, CT, and MRI, often cannot distinguish healthy from malignant tissue following therapy due to therapy induced changes in tissue structure (68,69). The only definitive way to determine if residual or recurrent tissue is malignant is the histological analysis of random biopsies, which are subject to sampling errors and are more difficult to pathologically interpret after therapy.

The spectroscopic criteria used to identify residual/recurrent prostate cancer needs to be adjusted due to a time dependent loss of prostate metabolites following therapy. For example, prostatic citrate production and secretion have been shown to be regulated by hormones (15), and an early dramatic reduction of citrate and polyamines after initiation of complete hormonal

blockade has been observed by MRSI (70). There was slower loss of choline and creatine with increasing duration of hormone deprivation therapy (70). This loss of prostatic metabolites correlates with the presence of tissue atrophy and is considered to be a indicator of effective therapy (70). Similar time dependent reductions in prostate metabolites also occurred after radiation therapy (71,72).

Studies have also demonstrated the ability of MRI/MRSI to discriminate residual or recurrent prostate cancer from residual benign tissue and atrophic/necrotic tissue after cryosurgery (73-75), hormone deprivation therapy (70,76) and radiation therapy (71,77). These studies have relied on elevated choline to creatine as a metabolic marker for prostate cancer since polyamines and citrate tend to disappear early after therapy in both residual healthy and malignant tissues. Figure 3B shows the same patient as in 3a, 4 years after therapy. Consistent with effective radiation therapy, there were a number of spectroscopic voxels that demonstrated a complete loss of all prostate metabolites (metabolic atrophy). However, residual metabolic abnormalities (choline to creatine ≥ 1.5) persisted bilaterally in the midgland towards the apex and this region was later confirmed as residual cancer by TRUS guided biopsy. A recent MRI/MRSI study of 21 prostate cancer patients with biochemical failure after external beam radiation therapy demonstrated that the presence of three or more voxels having a choline/creatine ≥ 1.5 in a hemiprostate showed a sensitivity and specificity of 87% and 72%, respectively, for the diagnosis of local cancer recurrence. The detection of residual cancer at an early stage following treatment and the ability to monitor the time course of therapeutic response would allow earlier intervention with additional therapy and provide a more quantitative assessment of therapeutic efficacy.

LIMITATIONS OF MRI/MRSI

Combined 1.5T MRI/MRSI has recognized limitations, including the potential for false positive and false negative results. The limitations include post-biopsy changes, confounding benign pathologies (prostatitis, BPH), mixing of cancer and healthy tissue with small volume (< 0.5 cc) early stage cancer and an insufficient understanding of the histological and biological basis of false positives and false negatives. Post-biopsy hemorrhage results in both over- and under-estimation of tumor extent at MRI and MRSI. (78-80). The timing of MRI and MRSI of the prostate following transrectal biopsy is therefore important. Early studies have recommended an interval of 3 weeks between transrectal biopsy and MR imaging (78-80). However, there has been a trend towards increased prostate sampling during transrectal biopsy; and currently greater than 6 core biopsies are frequently obtained (81). The increase in prostate sampling has raised new questions about the optimal timing of MRI and MRSI following transrectal biopsy, and the impact of post-biopsy hemorrhage on interpretation of MR and MRSI. In a recent study of 43 patients with biopsy-proven prostate cancer undergoing endorectal MRI and MRSI prior to radical prostatectomy confirming organ-confined disease, the outcome variables of capsular irregularity and spectral degradation were correlated with the predictor variables of time from biopsy and degree of post-biopsy hemorrhage (82). The authors found capsular irregularity was unrelated to time from biopsy or to degree of hemorrhage. Spectral degradation was inversely related to time from biopsy ($p < 0.01$); the mean percentage of degraded peripheral zone voxels was 18.5 % within 8 weeks of biopsy compared to 7 % after 8 weeks. Spectral degradation was unrelated to the degree of hemorrhage. The authors concluded that in organ-confined prostate cancer, capsular irregularity can be seen at any time after biopsy irrespective of the degree of hemorrhage, while spectral degradation is seen predominantly in the first 8 weeks. MR staging criteria and guidelines for scheduling studies after biopsy may require appropriate modification.

Only a few studies have investigated the MRI and MRSI appearances of acute and chronic prostatitis, but these initial reports suggest that in at least some cases prostatitis may mimic

cancer. Engelhard et al found that biopsy proven prostatitis correlated with areas of low T2 signal intensity at MRI (83). Theoretically, the inflammatory process of prostatitis might be expected to reduce the level of citrate seen at MRSI, although Van Dorsten et al failed to find any difference between healthy peripheral zone spectra and peripheral zone spectra from 12 patients thought to have prostatitis (84). Further studies with better pathological correlation are required to elucidate the true spectroscopic findings in prostatitis. Cancers within the central gland (transition zone and central zone) also have proven to be particularly difficult to discriminate on MRI/MRSI. There is significant overlap of low signal intensity on T_2 weighted images and metabolism on MRSI in regions of central gland tumor with predominately stromal Benign Prostatic Hyperplasia (BPH) (85). Regions of predominately glandular BPH have very elevated levels of citrate and polyamines since they are secretory products of healthy and hyperplastic glandular tissues. While in predominately stromal tissues, such as predominately stromal BPH, citrate and polyamine levels are very low similar to what is observed in cancer. Like cancer, there can also be somewhat elevated choline, since there is increased cellular proliferation in BPH as in cancer.

While prostatitis and stromal BPH are the most common benign confounding factors in over-calling prostate cancer by MRI/MRSI, prostate cancer can also be under-called due to signals arising from surrounding benign tissues masking the metabolic fingerprint of cancer, particularly for small infiltrative disease. Specifically, benign glandular tissues have very high signal intensity on T2 weighted MRI as well as very high levels of polyamines and citrate, and these signals will dominate the prostate spectrum. Predominately mucinogenic prostate cancer is also very difficult to detect on MRI/MRSI. On T2 weighted MRI they have high signal intensity due to the presence of the pockets of mucin. On MRSI, the spectral signal intensity is often very low due to the low density of prostate cancer cells.

FUTURE DIRECTIONS-HYPERPOLARIZED ^{13}C METABOLIC IMAGING OF THE PROSTATE

While the current commercially available clinical MRI/^{1}H MRSI prostate exam relies on changes in choline, citrate, and polyamine metabolism, lactate and alanine have largely been ignored due to the difficulty of suppressing the large signals from periprostatic lipids which overlap lactate and alanine (86). Significantly higher concentrations of lactate and alanine have been found in prostate cancer biopsies compared to healthy biopsy tissue. High levels of lactate in cancer is consistent with prior studies and has been associated with increased glycolysis and cell membrane biosynthesis (87,88). ^{18}F-2-deoxy-2-fluoro-D-glucose (FDG) positron emission tomography (PET) studies have shown high rates of glucose uptake in several human cancers and that the glucose uptake correlates directly with the aggressiveness of the disease and inversely with the patient's prognosis (89,90). The high glucose uptake leads to increased lactate production in most tumors even though some of them have sufficient oxygen, a condition know as the Warburg Effect (91) or aerobic glycolysis (87). The increased glycolysis provides the parasitic cancer cells with an energy source that is independent of its oxygen supply, a carbon source for the biosynthesis of cell membranes that begins with lipogenesis (88), and an acid source that likely enables the cells to invade neighboring tissue (87). New hyperpolarized ^{13}C spectroscopic imaging techniques (10,92,93) and advances in lipid suppression and spectral edited ^{1}H spectroscopic imaging (5,94) provide the opportunity to observe changes in lactate and alanine in clinical MRI/MRSI exams.

^{13}C labeled substrates have recently been polarized using dynamic nuclear polarization (DNP) techniques to obtain tens of thousands fold enhancement of the ^{13}C NMR signals from the substrate as well as its metabolic products (92,95,96). Preliminary DNP studies in rats, rat xenograft tumors, and a transgenic mouse model of prostate cancer (Figure 4) have demonstrated greater than 50,000-fold enhancements in the polarization of [1-^{13}C] pyruvate

and its metabolic products, lactate and alanine, providing sufficient MR signal for high spatial and temporal resolution spectroscopic imaging of the metabolites (10,93,97). Pyruvate is ideal for these studies because the signal from C-1 carbon relaxes very slowly as a result of its long T_1 and it is at the entry point to several important energy and biosynthesis pathways. In particular, it is converted to lactate in glycolysis, to alanine for protein synthesis and/or lipogenesis, and to acetyl-CoA and oxaloacetate to support the citric acid cycle and biosynthesis of membrane lipids. Several studies involving pre-clinical murine models of human prostate cancer have suggested that that hyperpolarized [^{13}C-1] lactate levels measured after the injection of hyperpolarized [^{13}C-1] pyruvate provide a non-invasive way to detect primary and metastatic disease and characterize the aggressiveness (histological stage) of prostate cancer (10,98) (Figure 4).

CONCLUSION

Commercial MRI/MRSI packages for staging prostate cancer on 1.5 T MR scanners are now available and the technology is becoming mature enough to begin assessing its clinical utility in large patient cohort studies using surgical pathology or clinical outcomes as the standard of reference. Prior to therapy, prostate cancer can be discriminated from benign tissues based on a combination of reduced signal intensity on T2 MRI, increased choline and reduced citrate and polyamines on MRSI. After therapy, the loss of all metabolites (metabolic atrophy) has been associated with effective therapy, while residual prostate cancer has been identified based on the presence of 3 or more voxels having Choline/Creatine > 1.5 with an accuracy of 80%. Recent studies have demonstrated that 1.5T MRI/MRSI has the potential to significantly improve the local evaluation of prostate cancer presence and volume and has been shown to have a significant incremental benefit in the prediction of pathological stage when added to nomograms incorporating non-imaging preoperative risk factors. Combined 1.5T MRI/MRSI also has recognized limitations, including the potential for false positive and false negative results, particularly for small volume (< 0.5 cc) early stage cancer. Recent studies have shown that accuracy can be improved by performing MRI/MRSI at higher magnetic field strengths (3T) (26,99), and through the addition of other functional MR techniques, namely DWI and DCE imaging (9). There are currently no commercially available 3T MRI/MRSI/DWI/DCE staging exams but the ability to accomplish this exam on clinical 3T scanners in a clinical reasonable time has been demonstrated and commercial products should be available within the next couple of years (9). Hyperpolarized ^{13}C labeled metabolic substrates have shown potential to revolutionize the way we use MRI in the risk assessment of prostate cancer patients (100,98,101). While pre-clinical hyperpolarized ^{13}C studies have been very encouraging, future studies are necessary to determine the feasibility of adding hyperpolarized ^{13}C spectroscopic imaging to a clinical multi-parametric MR staging exam of prostate cancer patients and for determining how all of the metabolic biomarkers can be best combined to provide the most accurate assessment of prostate cancer.

Acknowledgments

Grant Sponsors: National Institutes of Health: R01 CA102751; R01 CA111291, R01 EB007588, R01CA059897, R21 EB005363, R01 CA079980, University of California Discovery Grant: ITL-BIO04-10148

REFERENCES

1. Hricak H, White S, Vigneron D, et al. Carcinoma of the prostate gland: MR imaging with pelvic phased-array coils versus integrated endorectal--pelvic phased-array coils. Radiology 1994;193:703–709. [PubMed: 7972810]

2. Kurhanewicz J, Vigneron DB, Hricak H, Narayan P, Carroll P, Nelson SJ. Three-dimensional H-1 MR spectroscopic imaging of the in situ human prostate with high (0.24-0.7-cm3) spatial resolution. Radiology 1996;198:795–805. [PubMed: 8628874]

3. Tuan-Khanh CT, Vigneron DB, Sailasuta N, et al. Reducing Chemical Shift Errors and Conforming PRESS-CSI Selection with Very Selective Saturation (VSS) Pulses. JMRI. 1999
4. Schricker AA, Pauly JM, Kurhanewicz J, Swanson MG, Vigneron DB. Dualband spectral-spatial RF pulses for prostate MR spectroscopic imaging. Magn Reson Med 2001;46:1079–1087. [PubMed: 11746572]
5. Cunningham CH, Vigneron DB, Chen AP, et al. Design of symmetric-sweep spectral-spatial RF pulses for spectral editing. Magn Reson Med 2004;52:147–153. [PubMed: 15236378]
6. Wefer AE, Hricak H, Vigneron DB, et al. Sextant localization of prostate cancer: comparison of sextant biopsy, magnetic resonance imaging and magnetic resonance spectroscopic imaging with step section histology. J Urol 2000;164:400–404. [PubMed: 10893595]
7. Scheidler J, Hricak H, Vigneron DB, et al. Prostate cancer: localization with three-dimensional proton MR spectroscopic imaging--clinicopathologic study. Radiology 1999;213:473–480. [PubMed: 10551229]
8. Kurhanewicz J, Swanson MG, Nelson SJ, Vigneron DB. Combined magnetic resonance imaging and spectroscopic imaging approach to molecular imaging of prostate cancer. J Magn Reson Imaging 2002;16:451–463. [PubMed: 12353259]
9. Kurhanewicz J, Vigneron D, Carroll P, Coakley F. Multiparametric magnetic resonance imaging in prostate cancer: present and future. Curr Opin Urol 2008;18:71–77. [PubMed: 18090494]
10. Chen AP, Albers MJ, Cunningham CH, et al. Hyperpolarized C-13 spectroscopic imaging of the TRAMP mouse at 3T-Initial experience. Magn Reson Med 2007;58:1099–1106. [PubMed: 17969006]
11. Costello LC, Franklin RB. Concepts of citrate production and secretion by prostate. 1. Metabolic relationships. Prostate 1991;18:25–46. [PubMed: 1987578]
12. Costello LC, Franklin RB. Bioenergetic theory of prostate malignancy. Prostate 1994;25:162–166. [PubMed: 7520580]
13. Costello LC, Franklin RB. Novel role of zinc in the regulation of prostate citrate metabolism and its implications in prostate cancer. Prostate 1998;35:285–296. [PubMed: 9609552]
14. Franklin RB, Ma J, Zou J, et al. Human ZIP1 is a major zinc uptake transporter for the accumulation of zinc in prostate cells. J Inorg Biochem 2003;96:435–442. [PubMed: 12888280]
15. Costello LC, Franklin RB. Concepts of citrate production and secretion by prostate: 2. Hormonal relationships in normal and neoplastic prostate. Prostate 1991;19:181–205. [PubMed: 1946039]
16. Kahn T, Beurrig K, Schmitz-Dreager B, Lewin JS, Feurst G, Meodder U. Prostatic carcinoma and benign prostatic hyperplasia: MR imaging with histopathologic correlation. Radiology 1989;173:847–851. [PubMed: 2479050]
17. Schiebler ML, Tomaszewski JE, Bezzi M, et al. Prostatic carcinoma and benign prostatic hyperplasia: correlation of high-resolution MR and histopathologic findings. Radiology 1989;172:131–137. [PubMed: 2472644]
18. Liang JY, Liu YY, Zou J, Franklin RB, Costello LC, Feng P. Inhibitory effect of zinc on human prostatic carcinoma cell growth. Prostate 1999;40:200–207. [PubMed: 10398282]
19. Swanson MG, Vigneron DB, Tabatabai ZL, et al. Proton HR-MAS spectroscopy and quantitative pathologic analysis of MRI/3D-MRSI-targeted postsurgical prostate tissues. Magn Reson Med 2003;50:944–954. [PubMed: 14587005]
20. Swanson MG, Zektzer AS, Tabatabai ZL, et al. Quantitative analysis of prostate metabolites using (1)H HR-MAS spectroscopy. Magn Reson Med 2006;55:1257–1264. [PubMed: 16685733]
21. Ackerstaff E, Pflug BR, Nelson JB, Bhujwalla ZM. Detection of increased choline compounds with proton nuclear magnetic resonance spectroscopy subsequent to malignant transformation of human prostatic epithelial cells. Cancer Res 2001;61:3599–3603. [PubMed: 11325827]
22. Keshari, K.; Swanson, M.; Simko, J.; Vigneron, DB.; Nelson, S.; Kurhanewicz, J. Proc of the Intn'l Soc of Mag Res in Med. Berlin, Germany: 2007. Quantification of Choline and Ethanolamine Containing Phospholipids in Healthy and Malignant Prostate Tissue.
23. Saverio B, Pierpaola D, Serenella A, et al. Tumor progression is accompanied by significant changes in the levels of expression of polyamine metabolism regulatory genes and clusterin (sulfated glycoprotein 2) in human prostate cancer specimens. Cancer Research 2000;60:28–34. [PubMed: 10646846]

24. Swanson MG, Vigneron DB, Tran TK, Sailasuta N, Hurd RE, Kurhanewicz J. Single-voxel oversampled J-resolved spectroscopy of in vivo human prostate tissue. Magn Reson Med 2001;45:973–980. [PubMed: 11378874]
25. Heby O. Role of polyamines in the control of cell proliferation and differentiation. Differentiation 1981;19:1–20. [PubMed: 6173280]
26. Chen AP, Cunningham CH, Kurhanewicz J, et al. High-resolution 3D MR spectroscopic imaging of the prostate at 3 T with the MLEV-PRESS sequence. Magn Reson Imaging 2006;24:825–832. [PubMed: 16916699]
27. Carroll PR, Presti JJ, Small E, Roach Mr. Focal therapy for prostate cancer 1996: maximizing outcome. Urology 1997:84–94. [PubMed: 9123742]
28. Dhingsa R, Qayyum A, Coakley FV, et al. Prostate cancer localization with endorectal MR imaging and MR spectroscopic imaging: effect of clinical data on reader accuracy. Radiology 2004;230:215–220. [PubMed: 14695396]
29. Hasumi M, Suzuki K, Taketomi A, et al. The combination of multi-voxel MR spectroscopy with MR imaging improve the diagnostic accuracy for localization of prostate cancer. Anticancer Res 2003;23:4223–4227. [PubMed: 14666629]
30. Hasumi M, Suzuki K, Oya N, et al. MR spectroscopy as a reliable diagnostic tool for localization of prostate cancer. Anticancer Res 2002;22:1205–1208. [PubMed: 12168926]
31. Coakley FV, Kurhanewicz J, Lu Y, et al. Prostate cancer tumor volume: measurement with endorectal MR and MR spectroscopic imaging. Radiology 2002;223:91–97. [PubMed: 11930052]
32. Zakian KL, Sircar K, Hricak H, et al. Correlation of proton MR spectroscopic imaging with gleason score based on step-section pathologic analysis after radical prostatectomy. Radiology 2005;234:804–814. [PubMed: 15734935]
33. Weinreb J, Blume J, Coakley F, et al. Endorectal MR and MR spectroscopic imaging for sextant localization of prostate cancer prior to radical prostatectomy: Results of the ACRIN 6659 prospective multi-institutional clinicopathological study. Radiology. 2008Submitted
34. Villers A, Puech P, Mouton D, Leroy X, Ballereau C, Lemaitre L. Dynamic contrast enhanced, pelvic phased array magnetic resonance imaging of localized prostate cancer for predicting tumor volume: correlation with radical prostatectomy findings. J Urol 2006;176:2432–2437. [PubMed: 17085122]
35. D'Amico AV, Chang H, Holupka E, et al. Calculated prostate cancer volume: the optimal predictor of actual cancer volume and pathologic stage. Urology 1997;49:385–391. [PubMed: 9123703]
36. Smith JA Jr. Scardino PT, Resnick MI, Hernandez AD, Rose SC, Egger MJ. Transrectal ultrasound versus digital rectal examination for the staging of carcinoma of the prostate: results of a prospective, multi-institutional trial. J Urol 1997;157:902–906. [PubMed: 9072596]
37. Gleason D. Histologic Grading of Prostate Cancer: a Perspective. Human Pathology 1992;23:273–279. [PubMed: 1555838]
38. Wills ML, Sauvageot J, Partin AW, Gurganus R, Epstein JI. Ability of sextant biopsies to predict radical prostatectomy stage. Urology 1998;51:759–764. [PubMed: 9610589]
39. McLean M, Srigley J, Banerjee D, Warde P, Hao Y. Interobserver variation in prostate cancer Gleason scoring: are there implications for the design of clinical trials and treatment strategies? Clin Oncol (R Coll Radiol) 1997;9:222–225. [PubMed: 9315395]
40. Cooper JF, Farid I. The Role of Citric Acid in the Physiology of the Prostate. 3. Lactate/Citrate Ratios in Benign and Malignant Prostatic Homogenates as an Index of Prostatic Malignancy. J Urol 1964;92:533–536. [PubMed: 14226486]
41. Kurhanewicz J, Dahiya R, Macdonald JM, Chang LH, James TL, Narayan P. Citrate alterations in primary and metastatic human prostatic adenocarcinomas: 1H magnetic resonance spectroscopy and biochemical study. Magn Reson Med 1993;29:149–157. [PubMed: 8429778]
42. Kurhanewicz J, Vigneron DB, Nelson SJ. Three-dimensional magnetic resonance spectroscopic imaging of brain and prostate cancer. Neoplasia 2000;2:166–189. [PubMed: 10933075]
43. Yu KK, Hricak H, Alagappan R, Chernoff DM, Bacchetti P, Zaloudek CJ. Detection of extracapsular extension of prostate carcinoma with endorectal and phased-array coil MR imaging: multivariate feature analysis. Radiology 1997;202:697–702. [PubMed: 9051019]

44. Yu KK, Scheidler J, Hricak H, et al. Prostate cancer: prediction of extracapsular extension with endorectal MR imaging and three-dimensional proton MR spectroscopic imaging. Radiology 1999;213:481–488. [PubMed: 10551230]
45. Partin AW, Yoo J, Carter HB, et al. The use of prostate specific antigen, clinical stage and Gleason score to predict pathological stage in men with localized prostate cancer. J Urol 1993;150:110–114. [PubMed: 7685418]
46. Graefen M, Augustin H, Karakiewicz PI, et al. Can predictive models for prostate cancer patients derived in the United States of America be utilized in European patients? A validation study of the Partin tables. Eur Urol 2003;43:6–10. [PubMed: 12507538]discussion 11
47. Steyerberg EW, Roobol MJ, Kattan MW, van der Kwast TH, de Koning HJ, Schroder FH. Prediction of indolent prostate cancer: validation and updating of a prognostic nomogram. J Urol 2007;177:107–112. [PubMed: 17162015]discussion 112
48. Wang L, Hricak H, Kattan MW, et al. Prediction of seminal vesicle invasion in prostate cancer: incremental value of adding endorectal MR imaging to the Kattan nomogram. Radiology 2007;242:182–188. [PubMed: 17090712]
49. Wang L, Hricak H, Kattan MW, Chen HN, Scardino PT, Kuroiwa K. Prediction of organ-confined prostate cancer: incremental value of MR imaging and MR spectroscopic imaging to staging nomograms. Radiology 2006;238:597–603. [PubMed: 16344335]
50. Han M, Partin AW, Piantadosi S, Epstein JI, Walsh PC. Era specific biochemical recurrence-free survival following radical prostatectomy for clinically localized prostate cancer. J Urol 2001;166:416–419. [PubMed: 11458039]
51. Draisma G, Boer R, Otto SJ, et al. Lead times and overdetection due to prostate-specific antigen screening: estimates from the European Randomized Study of Screening for Prostate Cancer. J Natl Cancer Inst 2003;95:868–878. [PubMed: 12813170]
52. Etzioni R, Penson DF, Legler JM, et al. Overdiagnosis due to prostate-specific antigen screening: lessons from U.S. prostate cancer incidence trends. J Natl Cancer Inst 2002;94:981–990. [PubMed: 12096083]
53. Carroll PR. Early stage prostate cancer--do we have a problem with over-detection, overtreatment or both? J Urol 2005;173:1061–1062. [PubMed: 15758699]
54. Coakley FV, Hricak H. Radiologic anatomy of the prostate gland: a clinical approach. Radiologic Clinics of North America 2000;38:15–30. [PubMed: 10664664]
55. Prando A, Kurhanewicz J, Borges AP, Oliveira EM Jr. Figueiredo E. Prostatic biopsy directed with endorectal MR spectroscopic imaging findings in patients with elevated prostate specific antigen levels and prior negative biopsy findings: early experience. Radiology 2005;236:903–910. [PubMed: 16118169]
56. Yuen JS, Thng CH, Tan PH, et al. Endorectal magnetic resonance imaging and spectroscopy for the detection of tumor foci in men with prior negative transrectal ultrasound prostate biopsy. J Urol 2004;171:1482–1486. [PubMed: 15017203]
57. Westphalen AC, McKenna DA, Kurhanewicz J, Coakley FV. Role of magnetic resonance imaging and magnetic resonance spectroscopic imaging before and after radiotherapy for prostate cancer. J Endourol 2008;22:789–794. [PubMed: 18366322]
58. Sannazzari GL, Ragona R, Redda MG Ruo, Giglioli FR, Isolato G, Guarneri A. CT-MRI image fusion for delineation of volumes in three-dimensional conformal radiation therapy in the treatment of localized prostate cancer. Br J Radiol 2002;75:603–607. [PubMed: 12145134]
59. Pickett B, Vigneault E, Kurhanewicz J, Verhey L, Roach M. Static field intensity modulation to treat a dominant intra-prostatic lesion to 90 Gy compared to seven field 3-dimensional radiotherapy. Int J Radiat Oncol Biol Phys 1999;44:921–929. [PubMed: 10386651]
60. van Lin EN, Futterer JJ, Heijmink SW, et al. IMRT boost dose planning on dominant intraprostatic lesions: gold marker-based three-dimensional fusion of CT with dynamic contrast-enhanced and 1H-spectroscopic MRI. Int J Radiat Oncol Biol Phys 2006;65:291–303. [PubMed: 16618584]
61. Xia P, Pickett B, Vigneault E, Verhey LJ, Roach M 3rd. Forward or inversely planned segmental multileaf collimator IMRT and sequential tomotherapy to treat multiple dominant intraprostatic lesions of prostate cancer to 90 Gy. Int J Radiat Oncol Biol Phys 2001;51:244–254. [PubMed: 11516874]

62. DiBiase SJ, Hosseinzadeh K, Gullapalli RP, et al. Magnetic resonance spectroscopic imaging-guided brachytherapy for localized prostate cancer. Int J Radiat Oncol Biol Phys 2002;52:429–438. [PubMed: 11872289]
63. Pouliot J, Kim Y, Lessard E, Hsu IC, Vigneron DB, Kurhanewicz J. Inverse planning for HDR prostate brachytherapy used to boost dominant intraprostatic lesions defined by magnetic resonance spectroscopy imaging. Int J Radiat Oncol Biol Phys 2004;59:1196–1207. [PubMed: 15234056]
64. Zaider M, Zelefsky MJ, Lee EK, et al. Treatment planning for prostate implants using magnetic-resonance spectroscopy imaging. Int J Radiat Oncol Biol Phys 2000;47:1085–1096. [PubMed: 10863082]
65. Kim Y, Hsu IC, Lessard E, Kurhanewicz J, Noworolski SM, Pouliot J. Class solution in inverse planned HDR prostate brachytherapy for dose escalation of DIL defined by combined MRI/MRSI. Radiother Oncol. 2007
66. Blasko JC, Wallner K, Grimm PD, Ragde H. Prostate specific antigen based disease control following ultrasound guided 125iodine implantation for stage T1/T2 prostatic carcinoma. J Urol 1995;154:1096–1099. [PubMed: 7543606]
67. Zagars GK, Pollack A. External beam radiotherapy dose response of prostate cancer. Int J Radiat Oncol Biol Phys 1997;39:1011–1018. [PubMed: 9392538]
68. Coakley FV, Hricak H, Wefer AE, Speight JL, Kurhanewicz J, Roach M. Brachytherapy for prostate cancer: endorectal MR imaging of local treatment-related changes. Radiology 2001;219:817–821. [PubMed: 11376276]
69. Chen M, Hricak H, Kalbhen CL, et al. Hormonal ablation of prostatic cancer: effects on prostate morphology, tumor detection, and staging by endorectal coil MR imaging. AJR Am J Roentgenol 1996;166:1157–1163. [PubMed: 8615261]
70. Mueller-Lisse UG, Swanson MG, Vigneron DB, et al. Time-dependent effects of hormone-deprivation therapy on prostate metabolism as detected by combined magnetic resonance imaging and 3D magnetic resonance spectroscopic imaging. Magn Reson Med 2001;46:49–57. [PubMed: 11443710]
71. Roach M 3rd, Kurhanewicz J, Carroll P. Spectroscopy in prostate cancer: hope or hype? Oncology (Williston Park) 2001;15:1399–1410. [PubMed: 11758871]discussion 1415-1396, 1418
72. Pickett B, Ten Haken RK, Kurhanewicz J, et al. Time to metabolic atrophy after permanent prostate seed implantation based on magnetic resonance spectroscopic imaging. Int J Radiat Oncol Biol Phys 2004;59:665–673. [PubMed: 15183469]
73. Kalbhen CL, Hricak H, Chen M, et al. Prostate carcinoma: MR imaging findings after cryosurgery. Radiology 1996;198:807–811. [PubMed: 8628875]
74. Parivar F, Hricak H, Shinohara K, et al. Detection of locally recurrent prostate cancer after cryosurgery: evaluation by transrectal ultrasound, magnetic resonance imaging, and three-dimensional proton magnetic resonance spectroscopy. Urology 1996;48:594–599. [PubMed: 8886066]
75. Parivar F, Kurhanewicz J. Detection of recurrent prostate cancer after Cryosurgery. Current Opinion in Urology 1998;8:83–86. [PubMed: 17035847]
76. Mueller-Lisse UG, Vigneron DB, Hricak H, et al. Localized prostate cancer: Effect of hormone deprivation therapy measured by using combined three-dimensional H-1 MR spectroscopy and MR imaging: Clinicopathologic case-controlled study. Radiology 2001;221:380–390. [PubMed: 11687679]
77. Pickett B, Kurhanewicz J, Coakley F, Shinohara K, Fein B, Roach M 3rd. Use of MRI and spectroscopy in evaluation of external beam radiotherapy for prostate cancer. Int J Radiat Oncol Biol Phys 2004;60:1047–1055. [PubMed: 15519774]
78. Chelsky MJ, Schnall MD, Seidmon EJ, Pollack HM. Use of endorectal surface coil magnetic resonance imaging for local staging of prostate cancer. J Urol 1993;150(2 Pt 1):391–395. [PubMed: 8326561]
79. Schnall MD, Imai Y, Tomaszewski J, Pollack HM, Lenkinski RE, Kressel HY. Prostate cancer: local staging with endorectal surface coil MR imaging. Radiology 1991;178:797–802. [PubMed: 1994421]
80. White S, Hricak H, Forstner R, et al. Prostate cancer: effect of postbiopsy hemorrhage on interpretation of MR images. Radiology 1995;195:385–390. [PubMed: 7724756]

81. Bauer JJ, Zeng J, Zhang W, et al. Lateral biopsies added to the traditional sextant prostate biopsy pattern increases the detection rate of prostate cancer. Prostate Cancer Prostatic Dis 2000;3:43–46. [PubMed: 12497161]
82. Qayyum A, Coakley FV, Lu Y, et al. Organ-Confined Prostate Cancer: Effect of Prior Transrectal Biopsy on Endorectal MRI and MR Spectroscopic Imaging. AJR Am J Roentgenol 2004;183:1079–1083. [PubMed: 15385308]
83. Engelhard K, Hollenbach HP, Deimling M, Kreckel M, Riedl C. Combination of signal intensity measurements of lesions in the peripheral zone of prostate with MRI and serum PSA level for differentiating benign disease from prostate cancer. Eur Radiol 2000;10:1947–1953. [PubMed: 11305577]
84. van Dorsten FA, van der Graaf M, Engelbrecht MR, et al. Combined quantitative dynamic contrast-enhanced MR imaging and (1)H MR spectroscopic imaging of human prostate cancer. J Magn Reson Imaging 2004;20:279–287. [PubMed: 15269954]
85. Zakian KL, Eberhardt S, Hricak H, et al. Transition zone prostate cancer: metabolic characteristics at 1H MR spectroscopic imaging--initial results. Radiology 2003;229:241–247. [PubMed: 12920178]
86. Nelson SJ, Vigneron DB, Star-Lack J, Kurhanewicz J. High spatial resolution and speed in MRSI. NMR Biomed 1997;10:411–422. [PubMed: 9542738]
87. Gatenby RA, Gillies RJ. Why do cancers have high aerobic glycolysis? Nat Rev Cancer 2004;4:891–899. [PubMed: 15516961]
88. Costello LC, Franklin RB. 'Why do tumour cells glycolyse?': from glycolysis through citrate to lipogenesis. Mol Cell Biochem 2005;280:1–8. [PubMed: 16511951]
89. Mochiki E, Kuwano H, Katoh H, Asao T, Oriuchi N, Endo K. Evaluation of 18F-2-deoxy-2-fluoro-D-glucose positron emission tomography for gastric cancer. World J Surg 2004;28:247–253. [PubMed: 14961197]
90. Kunkel M, Reichert TE, Benz P, et al. Overexpression of Glut-1 and increased glucose metabolism in tumors are associated with a poor prognosis in patients with oral squamous cell carcinoma. Cancer 2003;97:1015–1024. [PubMed: 12569601]
91. Warburg O, Wind F, Negelein E. Uber den Stoffwechsel von Tumouren im Korper. Klin Woch 1926;5:829–832.
92. Ardenkjaer-Larsen JH, Fridlund B, Gram A, et al. Increase in signal-to-noise ratio of > 10,000 times in liquid-state NMR. Proc Natl Acad Sci U S A 2003;100:10158–10163. [PubMed: 12930897]
93. Kohler SJ, Yen Y, Wolber J, et al. In vivo (13)carbon metabolic imaging at 3T with hyperpolarized (13)C-1-pyruvate. Magn Reson Med 2007;58:65–69. [PubMed: 17659629]
94. Star-Lack J, Spielman D, Adalsteinsson E, Kurhanewicz J, Terris DJ, Vigneron DB. In vivo lactate editing with simultaneous detection of choline, creatine, NAA, and lipid singlets at 1.5 T using PRESS excitation with applications to the study of brain and head and neck tumors. J Magn Reson 1998;133:243–254. [PubMed: 9716465]
95. Golman K, Olsson LE, Axelsson O, Mansson S, Karlsson M, Petersson JS. Molecular imaging using hyperpolarized 13C. Br J Radiol 2003;76 Spec No 2:S118–127. [PubMed: 15572334]
96. Mansson S, Johansson E, Magnusson P, et al. 13C imaging-a new diagnostic platform. Eur Radiol 2006;16:57–67. [PubMed: 16402256]
97. Golman K, Zandt RI, Lerche M, Pehrson R, Ardenkjaer-Larsen JH. Metabolic imaging by hyperpolarized 13C magnetic resonance imaging for in vivo tumor diagnosis. Cancer Res 2006;66:10855–10860. [PubMed: 17108122]
98. Albers, MJ.; Chen, AP.; Bok, R., et al. Monitoring Prostate Cancer Progression in A Transgenic Murine Model Using 3T Hyperpolarized 13C MRS. ISMRM Fifteenth Scientific Meeting; Berlin, Germany. 2007;
99. Cunningham CH, Vigneron DB, Marjanska M, et al. Sequence design for magnetic resonance spectroscopic imaging of prostate cancer at 3 T. Magn Reson Med 2005;53:1033–1039. [PubMed: 15844147]
100. Golman K, Ardenaer-Larsen JH, Petersson JS, Mansson S, Leunbach I. Molecular imaging with endogenous substances. Proceedings of the National Academy of Sciences of the United States of America 2003;100:10435–10439. [PubMed: 12930896]

101. Cunningham CH, Chen AP, Albers MJ, et al. Double spin-echo sequence for rapid spectroscopic imaging of hyperpolarized (13)C. J Magn Reson 2007;187:357–362. [PubMed: 17562376]

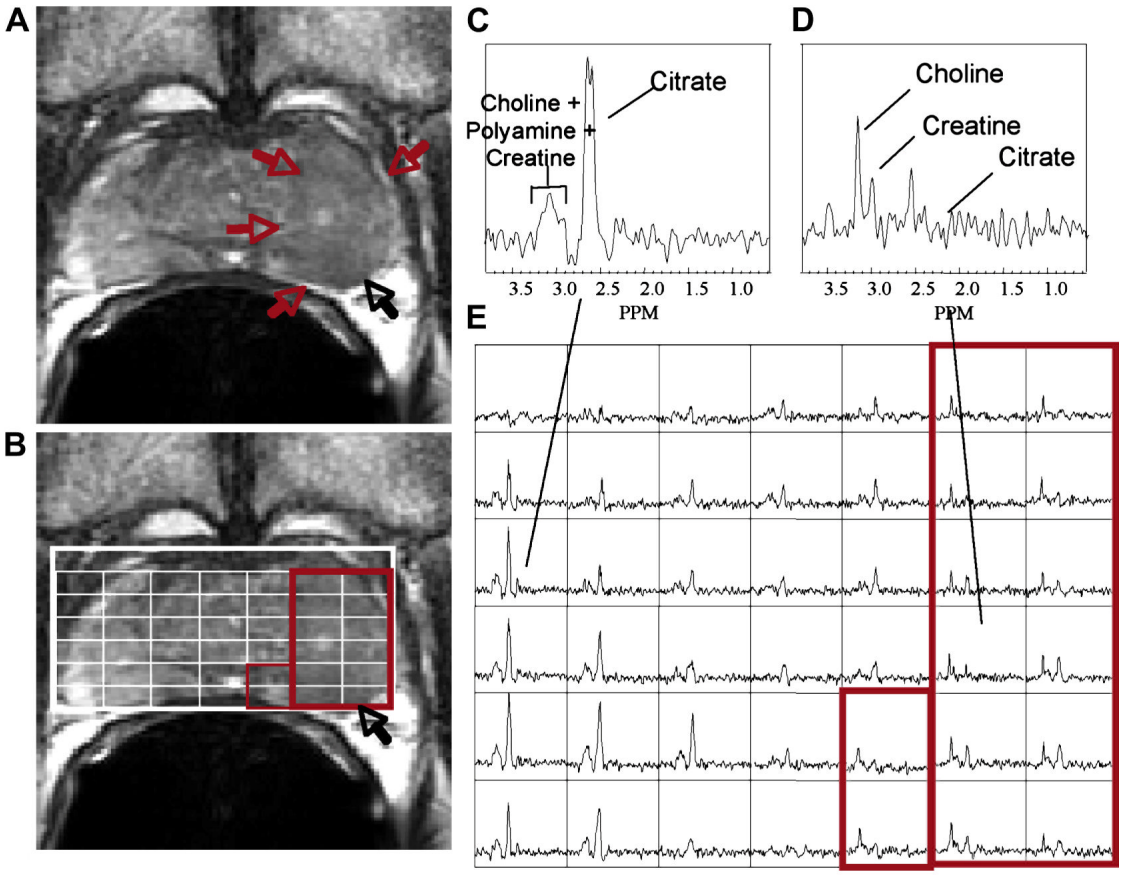

Figure 1.

(a) A) A reception-profile corrected T2 weighted FSE axial image taken from a volume MRI/MRSI data set demonstrating a large region of hypointensity in the left midgland (red arrows) with suspected extracapsular extension (black arrow). The selected volume for spectroscopy (bold white box) and a portion of the 16 × 8 × 8 spectral phase encode grid overlaid (fine white line) on the T2 weighted image (B) with the corresponding 0.3 cm^3 proton spectral array (E). Spectra in regions of cancer (D, red box) demonstrate dramatically elevated choline, an absence of citrate and polyamines relative to regions of healthy peripheral zone tissue (C). In this fashion, metabolic abnormalities can be correlated with anatomic abnormalities from throughout the prostate. The strength of the combined MRI/MRSI exam has been found to be when changes in all three metabolic markers (choline, polyamines and citrate) and imaging findings are concordant for cancer.

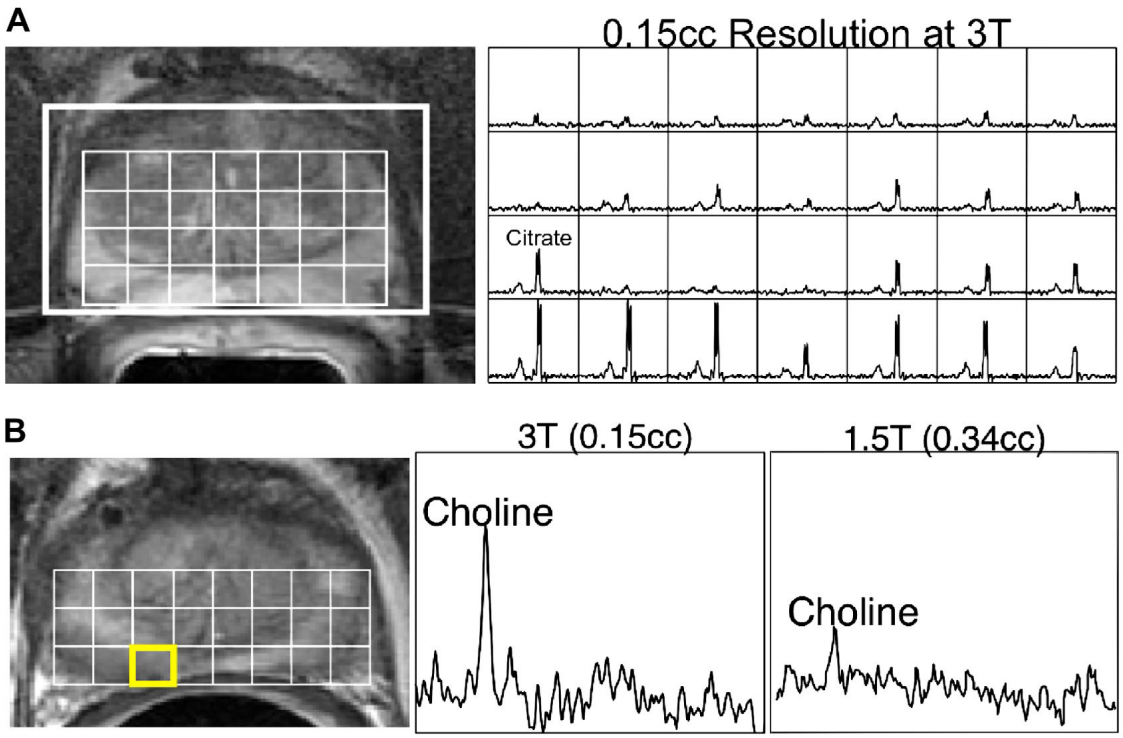

Figure 2.

Prostate MRI/MRSI data obtained on a 3 Tesla scanner with the j-refocused, MLEV-PRESS (Point RESolved Spectroscopy) MRSI sequence (101). A) T_2-weighted MRI and a 3D MR spectral array are shown for a pre-therapy patient. The 3D MRSI data were acquired in 17 minutes with a spatial resolution of 0.15 cm^3 using the specialized acquisition sequence to obtain upright citrate resonances at an echo time of 85ms on a 3 Tesla MR scanner. B) 3T MRI and MRSI data are shown for the same prostate cancer patient with biopsy proven cancer in the right midgland. The higher resolution obtainable at 3T MRSI (middle) depicted more clearly the elevated choline levels as compared to the corresponding 1.5T data (right) acquired on the same day.

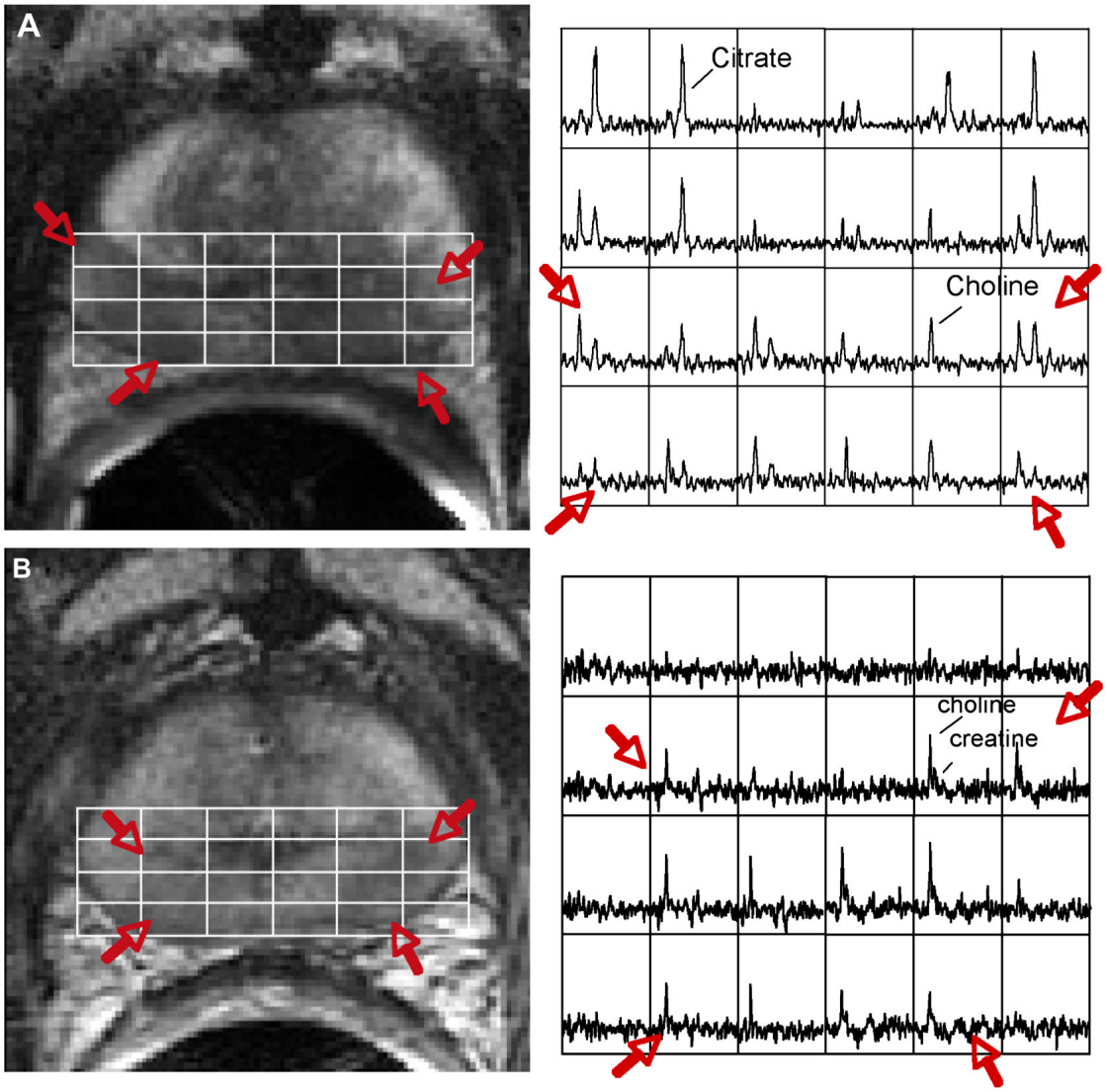

Figure 3.

(A) Endorectal coil Fast Spin Echo T2 weighted image from the midgland of prostate demonstrating bilateral low signal intensity (red arrows) in the regions of biopsy proven prostate cancer. The overlying white grid shows the locations where the MRSI spectra are taken from (right). Regions of prostate cancer (red arrow) demonstrate elevated choline and reduced citrate relative to regions of healthy tissue. (B) A T2 weighted image and corresponding spectral array taken from the same location as in (A) four years after combined radiation and androgen deprivation therapy. There are a number of voxels demonstrating metabolic atrophy consistent with effective treatment; however, there remain bilateral regions of elevated choline that was confirmed to be recurrent prostate cancer at biopsy.

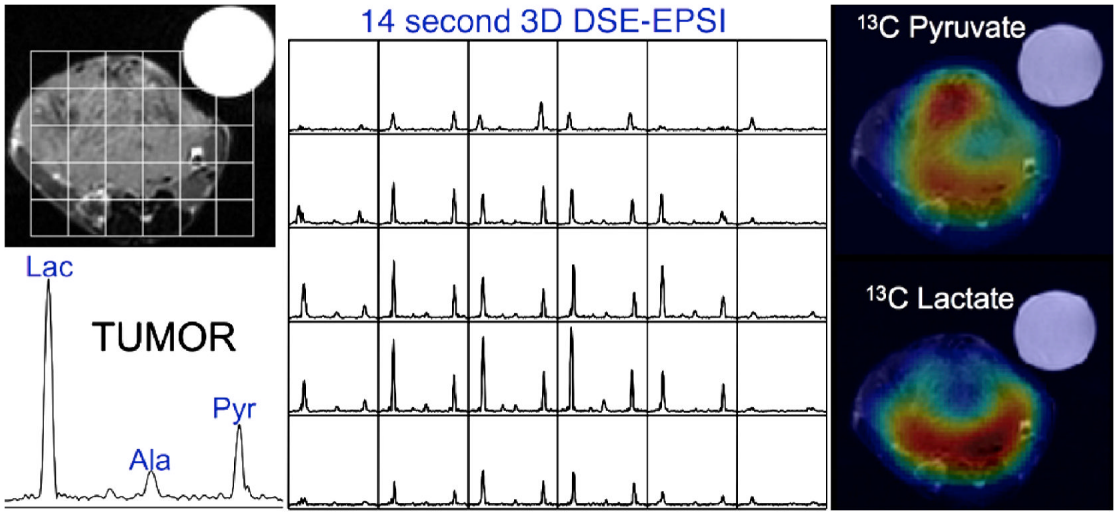

Figure 4.

This study of a TRAMP prostate model tumor using the HyperSense system for pre-polarization demonstrated not only high ^{13}C lactate in the tumor but also differences in metabolite distributions in the tumor. The data were acquired in 14 seconds and show high uptake of hyperpolarized pyruvate throughout much of the tumor, except for a presumably necrotic region at the center. The lactate image demonstrated a focus of high metabolic activity in the posterior aspect of the tumor, which is indicative of biologically aggressive cancer.